The Stability of Large-Amplitude Shallow Interfacial Non-Boussinesq Flows

By Anakewit Boonkasame and Paul Milewski

The system of equations describing the shallow-water limit dynamics of the interface between two layers of immiscible fluids of different densities is formulated. The flow is bounded by horizontal top and bottom walls. The resulting equations are of mixed type: hyperbolic when the shear is weak and the behavior of the system is internal-wave like, and elliptic for strong shear. This ellipticity, or ill-posedness is shown to be a manifestation of large-scale shear instability. This paper gives sharp nonlinear stability conditions for this nonlinear system of equations. For initial data that are initially hyperbolic, two different types of evolution may occur: the system may remain hyperbolic up to internal wave breaking, or it may become elliptic prior to wave breaking. Using simple waves that give *a priori* bounds on the solutions, we are able to characterize the condition preventing the second behavior, thus providing a long-time well-posedness, or nonlinear stability result. Our formulation also provides a systematic way to pass to the Boussinesq limit, whereby the density differences affect buoyancy but not momentum, and to recover the result that shear instability cannot occur from hyperbolic initial data in that case.

1. Introduction

Density-stratified fluids are ubiquitous in nature, with the ocean and the atmosphere as examples of interest. One of the simplest configurations of stratified flows is that of two layers of ideal fluids with different densities

Address for correspondence: Paul Milewski, Department of Mathematics, University of Wisconsin-Madison, 480 Lincoln Drive, Madison, WI 53706, USA; e-mail: milewski@math.wisc.edu

DOI: 10.1111/j.1467-9590.2011.00528.x

STUDIES IN APPLIED MATHEMATICS 0:1–19

bounded by flat horizontal walls. We consider the two-dimensional problem only, and thus the interface between the fluids is a curve. The modeling of the problem can be simplified by considering two approximations to the Euler equations and interfacial boundary conditions: (i) the long-wave limit, which assumes that the horizontal length scale of motion is much longer than the depth of both fluids, and (ii) the Boussinesq approximation, which assumes that the density difference between the two fluids is small and contributes only to the relative buoyancy of the fluids, not to their inertia. These limits have been introduced and investigated in a number of previous works including, for example [1–3]. The first assumption results, at leading order, in a system of first-order nonlinear partial differential equations (with, possibly, a nonlocal pressure equation) of mixed type. An important aspect of this system is that of *well-posedness*, which corresponds physically to whether the behavior is *wave-like* or whether a violent Kelvin–Helmholtz (KH) instability in the full Euler problem is dominant, and which is mathematically related to whether the system is *hyperbolic* or elliptic. The strongest result one can show is that the system is well posed "globally," meaning that it remains in a hyperbolic regime for all time (up to breaking). Local well-posedness for a class of three-dimensional systems, including the one considered here when restricted to the two-dimensional case, was proved in [GLS] and [4, 5]. Well-posedness can also be thought of as a *stability* result because it answers the question of whether violent KH instability—instability on a length scale comparable to the depth of the fluid—will arise out of wave-like behavior.

The stability of stratified shear flows can be characterized by a local *Richardson number*, which compares the effects of buoyancy with shear. In the present case the Richardson number is defined as

$$Ri = gH\frac{\delta\rho/\bar{\rho}}{(u_2-u_1)^2}\times\frac{\bar{\rho}}{H}\left(\frac{h_2}{\rho_2}+\frac{h_1}{\rho_1}\right),$$

where u_j are the horizontal velocities, h_j the layer depths, ρ_j the densities, and $j = 1, 2$ denote the upper and lower layers, respectively. The total depth is H, the mean density is denoted by $\bar{\rho}$, the density difference $\delta\rho$, and g is the acceleration due to gravity. If $Ri > 1$, the two-layer shallow-water system is hyperbolic. For future reference, note that under the Boussinesq approximation, the second factor in the Richardson number above is identically 1.

In [6, 7], it was shown that, under the Boussinesq approximation, the shallow-water evolution is globally stable. In other words, given initial data $u_j(x)$, $h_j(x)$ such that $Ri > 1$ everywhere, the evolution will remain hyperbolic, that is, preserving $Ri > 1$, and will consist of internal waves that ultimately break. The present work extends this type of global stability result to the more general system obtained without the Boussinesq approximation. We show that in this case, certain hyperbolic initial data *may become KH unstable*, resulting in $Ri < 1$, and we provide a *sharp* characterization of initial data that will not lead to shear instability. These results are obtained through *simple waves* of

the system [8]. One straightforward consequence of the present work is a choice of variables that yields the Boussinesq approximation systematically as the density difference between the layers tends to zero.

Our use of the term stability requires some explanation. It is well known [9] that, in the absence of surface tension, the horizontal interface between two fluids of different densities with different horizontal velocities is *always* KH unstable at sufficiently short wavelengths (even at arbitrarily small shear). The long-wave approximation in this and other studies (e.g. [10, 11]) filters out short-scale dynamics, thus taming this instability. Physically, while this instability may be present at the small scales, it does not substantially affect the large-scale motion; it either generates a more complex interface at the small scales or serves to locally mix the fluid in a small region near the interface, yielding a continuous density and shear profile. We conjecture that large-scale waves propagate largely unaffected by these small-scale phenomena, a fact that has been tested in solitary wave profiles [12]. As the shear is increased and $Ri < 1$, the KH instability occurs at longer spatial scales comparable to the distance between the bounding walls, and this is reflected in the shallow-water equations, making them elliptic.

In the Boussinesq approximation, $Ri = 1$ coincides with the point at which there is sufficient kinetic energy in the shear to "mix" the fluid layers [7]. (That is, there is sufficient energy to overcome the potential energy barrier to mix the fluids.) One can therefore expect that when $Ri < 1$ the instability will be strong enough that the sharp interface no longer has real meaning. Although mixing is not discussed further, it is worth emphasizing that mixing of fluids either due to wave breaking (hydraulic jumps) or the KH instability is an important process in geophysical stratified flows and is ultimately an ingredient of the stratification profile itself. In the context of shallow-water flows, systematic closures for mixing at internal shocks were developed in [13, 14].

This paper is organized as follows. In Section 2, a system of equations describing the problem is derived from first principles, together the Boussinesq limit obtained in a systematic manner. The simplified system resulting from this approximation serves as a starting point for the study of nonlinear stability in Section 3. In Section 4, the notion of simple waves is introduced and used to obtain bounds on the solution that yield a sharp stability result.

2. Formulation

Consider irrotational flow in two layers of immiscible, incompressible, ideal fluids bounded by horizontal top and bottom walls as shown in Figure 1. Let H be the separation between the walls and L be the typical horizontal length scale of the fluid motion, and define $\mu \equiv H/L$ as the long-wave parameter.

The nondimensionalized quantities (with their scaling shown in brackets) are:

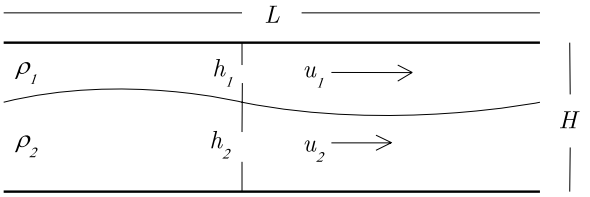

Figure 1. Two layers of immiscible fluids bounded by horizontal top and bottom walls.

- H_1, H_2 $[\times H]$ for heights of undisturbed fluid layers,
- ρ_1, ρ_2 $[\times \bar{\rho}]$ for densities of the fluids,
- x $[\times L]$ for horizontal position,
- y $[\times H]$ for vertical position measured from undisturbed interface,
- τ $[\times L/\sqrt{gH}]$ for time,
- h_1, h_2 $[\times H]$ for heights of fluid layers,
- u_1, u_2 $[\times \sqrt{gH}]$ for horizontal components of fluid velocities,
- v_1, v_2 $[\times \mu\sqrt{gH}]$ for vertical components of fluid velocities,
- P_1, P_2 $[\times \bar{\rho} gH]$ for pressures.

The nondimensional governing equations in each layer are:

$$u_{j,x} + v_{j,y} = 0, \tag{1}$$

$$\mu^2 v_{j,x} - u_{j,y} = 0, \tag{2}$$

$$u_{j,\tau} + \left(u_j^2\right)_x + (v_j u_j)_y = -\frac{P_{j,x}}{\rho_j}, \tag{3}$$

$$\mu^2\left[v_{j,\tau} + (u_j v_j)_x + \left(v_j^2\right)_y\right] = -\frac{P_{j,y}}{\rho_j} - 1. \tag{4}$$

On the top and bottom walls, the vertical velocity vanishes:

$$v_1 = 0 \quad \text{for} \quad y = H_1 \quad \text{and} \quad v_2 = 0 \quad \text{for} \quad y = -H_2. \tag{5}$$

At the interface $y = H_1 - h_1 = h_2 - H_2$, the boundary conditions are the kinematic conditions:

$$h_{1,\tau} + h_{1,x}u_1 = -v_1 \quad \text{and} \quad h_{2,\tau} + h_{2,x}u_2 = v_2, \tag{6}$$

and the dynamic condition of continuity of pressure at the interface:

$$P_1 = P_2 \equiv P. \tag{7}$$

Conservation of mass (or volume) in each layer is obtained from (1), (5), and (6) by vertical averaging

$$h_{1\tau} + (h_1 \bar{u}_1)_x = 0, \tag{8}$$

$$h_{2\tau} + (h_2\bar{u}_2)_x = 0, \tag{9}$$

where

$$\bar{u}_1 = \frac{1}{h_1}\int_{H_1-h_1}^{H_1} u_1\,dy \quad \text{and} \quad \bar{u}_2 = \frac{1}{h_2}\int_{H_2}^{h_2-H_2} u_2\,dy.$$

Irrotationality (2) implies that $u_j = \bar{u}_j + O(\mu^2)$ and hence that $\overline{u_j^2} = \bar{u}_j^2 + O(\mu^4)$. (Note that some authors, e.g. [11], assume that $u_j = \bar{u}_j + O(\mu^2)$ without an explicit assumption of irrotationality.) Then from (3), (5), and (6), conservation of momentum is obtained:

$$\rho_1(\bar{u}_{1,\tau} + \bar{u}_1\bar{u}_{1,x} - h_{1,x}) = -P_x, \tag{10}$$

$$\rho_2(\bar{u}_{2,\tau} + \bar{u}_2\bar{u}_{2,x} + h_{2,x}) = -P_x. \tag{11}$$

Note that this pressure is unknown *a priori* and, to the order considered here, is related hydrostatically to the unknown pressure at the bottom and top walls by neglecting the left-hand side of (4). The systems (8)–(11) together with the constraint $h_1 + h_2 = 1$ govern the evolution of the fluid. We now reduce it to a system of two or three equations depending on certain conditions.

From (8) and (9), notice that $(h_1\bar{u}_1 + h_2\bar{u}_2)_x = 0$. Thus, the volume flux

$$Q(\tau) \equiv h_1\bar{u}_1 + h_2\bar{u}_2$$

is independent of x. In certain cases, Q is set by boundary conditions on the horizontal velocities. There are two situations for which Q is constant: (i) vertical sidewalls require that $Q = 0$ or (ii) far-field (inlet) conditions may fix Q to a time independent value. In general, however, using (8)–(11), one has the following relation between Q and P:

$$Q'(\tau) = -\left(h_1\bar{u}_1^2 + h_2\bar{u}_2^2 + \frac{h_2^2}{2} - \frac{h_1^2}{2}\right)_x - \left(\frac{h_1}{\rho_1} + \frac{h_2}{\rho_2}\right)P_x. \tag{12}$$

We now recast the system in terms of the variables $h \equiv h_2 - h_1$, $\tilde{w} \equiv \bar{u}_2 - \bar{u}_1$ and the "Boussinesq" parameter $r \equiv (\rho_2 - \rho_1)/2$, which indicates the strength of the stratification. Note that $-1 \le h \le 1$, $0 < r < 1$, $\rho_1 = 1 - r$ and $\rho_2 = 1 + r$. The quantity $\tilde{w}$ is the total shear between the two fluid layers. In these variables:

$$h_\tau + Qh_x + \left(\frac{(1-h^2)\tilde{w}}{2}\right)_x = 0,$$

$$\tilde{w}_\tau + Q\tilde{w}_x - \left(\frac{h\tilde{w}^2}{2}\right)_x = \frac{2rP_x}{1-r^2},$$

$$Q'(\tau) + \left(\frac{(1-h^2)\tilde{w}^2}{4} + \frac{h}{2}\right)_x = -\frac{(1-rh)P_x}{1-r^2}.$$

To take the Boussinesq limit in the next section, consider the rescalings $t \equiv \tau\sqrt{2r}$, $w \equiv \tilde{w}/\sqrt{2r}$, $q \equiv Q/\sqrt{2r}$, and the substitution

$$\frac{P}{1-r^2} = -\frac{h}{2} + rp.$$

The "deviation pressure" p is only significant in the non-Boussinesq case and has interesting properties. Under these substitutions, one obtains the system of equations

$$h_t + qh_x + \left(\frac{(1-h^2)w}{2}\right)_x = 0, \tag{13}$$

$$w_t + qw_x + \left(\frac{(1-w^2)h}{2}\right)_x = rp_x, \tag{14}$$

$$q'(t) + \left(\frac{(1-h^2)w^2}{4} + \frac{h^2}{8}\right)_x = -\frac{(1-rh)p_x}{2}. \tag{15}$$

The deviation pressure also depends on the boundary conditions. If q is constant, which is relevant in the physical situations mentioned above, one can use Equations (13) and (14) together with the pressure found from (15) with $q' = 0$. If, on the other hand, *periodic* boundary conditions are assumed, one can remove the pressure from (14) by dividing by $1 - rh$ and integrating over a spatial period, say $[-\pi, \pi]$, obtaining an equation for the time evolution of the volume flux

$$q'(t)\int_{-\pi}^{\pi} \frac{1}{1-rh}\,dx + \int_{-\pi}^{\pi} \frac{1}{1-rh}\left(\frac{(1-h^2)w^2}{4} + \frac{h^2}{8}\right)_x dx = 0. \tag{16}$$

This equation could then be used in (15) to express the deviation pressure. Note that the deviation pressure is always nonconservative, has a dynamic component, and, in the periodic case, is also nonlocal. The systems (13)–(15) may now be recast as the "non-Boussinesq system"

$$h_t + qh_x + \left(\frac{(1-h^2)w}{2}\right)_x = 0,$$

$$w_t + qw_x + \left(\frac{(1-w^2)h}{2}\right)_x + \frac{2r}{1-rh}\left(\frac{(1-h^2)w^2}{4} + \frac{h^2}{8}\right)_x = -\frac{2rq'(t)}{1-rh}.$$

The different cases are then obtained by setting either (i) $q = 0$ (sidewall conditions), (ii) $q = constant$ (far-field conditions) that may be reduced to the $q = 0$ case by using an appropriate reference frame, or (iii) q' from (16), resulting in a nonlocal system of equations.

2.1. Boussinesq approximation

We show that the Boussinesq approximation may be obtained from the equations derived by taking the limit $r = 0$. Consider first the simplified system obtained from making the approximation *a priori* by replacing the individual fluid densities with the mean density in the inertial terms of the Euler equations and retaining different densities in the buoyancy terms. A similar derivation as before shows that (10)–(12) become

$$\begin{aligned} \bar{u}_{1,\tau} + \bar{u}_1\bar{u}_{1,x} - \rho_1 h_{1,x} &= -P_x, \\ \bar{u}_{2,\tau} + \bar{u}_2\bar{u}_{2,x} + \rho_2 h_{2,x} &= -P_x, \\ Q'(\tau) + \left(h_1\bar{u}_1^2 + h_2\bar{u}_2^2 + \frac{h_2^2}{2} - \frac{h_1^2}{2}\right)_x &= -P_x. \end{aligned}$$

In all cases described in the prior section (including the periodic case), clearly, $Q'(\tau) = 0$. Thus one may set $Q = 0$ in an appropriate frame of reference, which allows, under the same definitions and rescaling as before, the reduction to the "Boussinesq system" of two equations

$$\begin{aligned} h_t + \left(\frac{(1-h^2)w}{2}\right)_x &= 0, \\ w_t + \left(\frac{(1-w^2)h}{2}\right)_x &= 0. \end{aligned}$$

Alternatively, the same equations can be obtained by setting $r = 0$ and $q = 0$ in the non-Boussinesq system of the prior section. In the Boussinesq case the deviation pressure is zero, and the pressure at the interface depends only on its height.

3. Stability

We first consider the simple linear stability analysis of uniform flows to set the context of the nonlinear, nonuniform results obtained later.

3.1. Linear stability

Consider the general situation shown in Figure 1and described by Equations (1)–(7). Performing the standard KH linear stability analysis [15] by perturbing the uniform state of constant h_1, h_2, u_1, u_2 and zero v_1, v_2 (a vortex sheet), one obtains modes with behavior in x and t proportional to $e^{i(kx-\omega t)}$, whose dispersion relation is given by

$$\mu[\rho_1(\omega - ku_1)^2 \cosh(\mu k h_1)\sinh(\mu k h_2) + \rho_2(\omega - ku_2)^2 \sinh(\mu k h_1)\cosh(\mu k h_2)] = (\rho_2 - \rho_1)k \sinh(\mu k h_1)\sinh(\mu k h_2),$$

where ω $[\times\sqrt{gH}/L]$ and k $[\times 1/L]$ are dimensionless.

At sufficiently small scales, obtained by fixing μ and taking kh_1, kh_2 large, the state is always linearly unstable, that is, ω has a positive imaginary part, if $u_1 - u_2 \neq 0$. This will result in small-scale instabilities at the interface regardless of the large-scale motion.

Upon taking the long-wave limit $\mu \to 0$, one obtains

$$\left[\omega - \frac{k(\rho_1 u_1 h_2 + \rho_2 u_2 h_1)}{\rho_1 h_2 + \rho_2 h_1}\right]^2 = \frac{k^2\left[(\rho_2 - \rho_1)h_1 h_2 - \rho_1 u_1^2 h_2 - \rho_2 u_2^2 h_1\right]}{\rho_1 h_2 + \rho_2 h_1} + \left[\frac{k(\rho_1 u_1 h_2 + \rho_2 u_2 h_1)}{\rho_1 h_2 + \rho_2 h_1}\right]^2. \tag{17}$$

Stability requires that the right-hand side of (17) be positive, which yields the equivalent conditions

$$Ri > 1 \quad \text{or} \quad |w| < \alpha(r, h) \equiv \sqrt{\frac{1 - rh}{1 - r^2}}. \tag{18}$$

This result is in agreement with that obtained in previous work, for example [16]. Thus, it is possible that long-wave motion is KH stable. We see that this is precisely the situation in which the system derived is locally hyperbolic.

3.2. Nonlinear stability for the Boussinesq system

The Boussinesq system is a quasi-linear system of mixed type and can be written in the standard form

$$u_t + B(u)u_x = 0, \tag{19}$$

where $u = (h, w)^\top$ and

$$B(u) = \begin{pmatrix} -hw & \dfrac{1 - h^2}{2} \\ \dfrac{1 - w^2}{2} & -hw \end{pmatrix}.$$

In order that (19) admits a wave-like solution, the system must be hyperbolic; that is, all eigenvalues of B must be real and its eigenvectors span $\mathbb{R}^2$ [17]. Because B has eigenvalues

$$\lambda_B^{\pm} = -hw \pm \frac{\sqrt{(1 - h^2)(1 - w^2)}}{2}$$

and corresponding eigenvectors

$$v_B^{\pm} = (\sqrt{1-h^2},\ \pm\sqrt{1-w^2})^{\top},$$

these conditions are satisfied for $|h| < 1$ and $|w| < 1$. (We exclude $|h| > 1$ and $|w| > 1$ as unphysical.) The square in the (h, w) phase space satisfying these inequalities is the *hyperbolic region*. Note that the second inequality agrees with (18) in the limit $r \to 0$.

In [7], *nonlinear stability* was defined as the property that any smooth solution of (19) evolving from initial data in the hyperbolic region remains in this region, and it was shown that a sufficient condition for a 2×2 quasi-linear system of mixed type to be nonlinearly stable is that its eigenvalues are smooth functions of its Riemann invariants on the boundary of the hyperbolic region. This is indeed the case for (19) because its Riemann invariants are explicitly computable:

$$R^{\pm} = \sqrt{(1-w^2)(1-h^2)} \mp wh,$$

and the eigenvalues are simple functions of the Riemann invariants:

$$\lambda_B^{+} = \frac{1}{4}(3R^{+} - R^{-}) \qquad \text{and} \qquad \lambda_B^{-} = \frac{1}{4}(R^{+} - 3R^{-}).$$

As an example, Figure 2 shows a numerical solution of (19) and its representation in the phase space. Different curves in the figures represent the solution at different times, with thick curves representing initial data. The final solution is at the time just before waves break. We assumed periodic boundary conditions, so the solution curves in the phase space are closed. Dashed lines are the boundaries of the hyperbolic region. Figure 3 shows another solution of (19) with initial data in close proximity of the top boundary of the hyperbolic

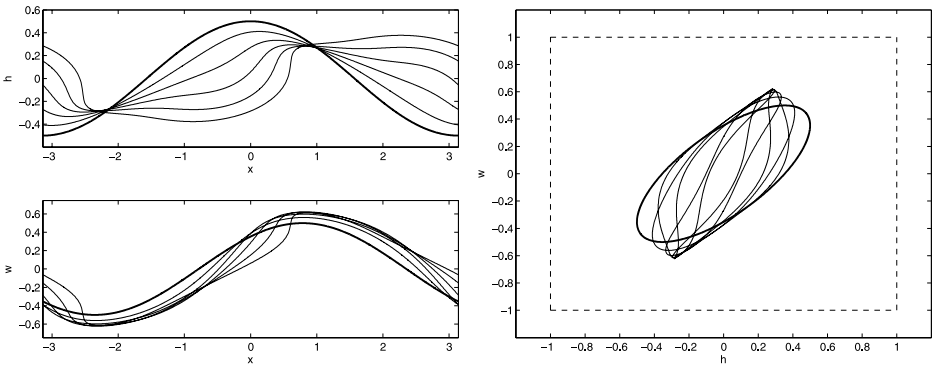

Figure 2. Typical solution of (19) up to breaking time; on the left, h and w are shown in physical space at various times. On the right, the evolution is shown in the phase space together with the boundary of the hyperbolic region.

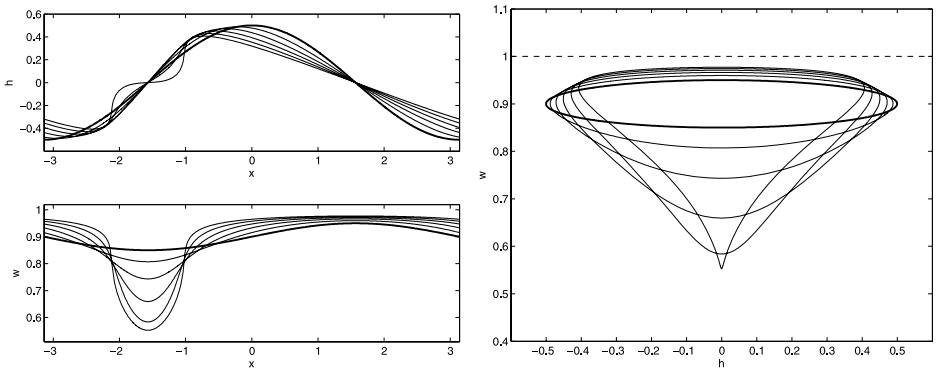

Figure 3. Solution of (19) up to breaking time with initial data near a boundary of the hyperbolic region.

region. Again, the solution remains in the hyperbolic region throughout its evolution.

3.3. *Nonlinear instability for the non-Boussinesq system*

In this section, contrasting computations to those of the previous section are presented. They illustrate that, in the non-Boussinesq setting, shallow-water instabilities *may* arise out of hyperbolic initial data.

The general non-Boussinesq system when $q'(t) = 0$—and without losing generality, setting $q = 0$—may be written

$$u_t + A(u)u_x = 0, \tag{20}$$

where

$$A(u) = \begin{pmatrix} -hw & \dfrac{1-h^2}{2} \\ \dfrac{1-(1+rh)w^2}{2(1-rh)} & \dfrac{(r-h)w}{1-rh} \end{pmatrix}.$$

The matrix A has eigenvalues

$$\lambda_A^{\pm} = \frac{(r-2h+rh^2)w \pm \sqrt{(1-r^2)(1-h^2)(\alpha(r,h)^2-w^2)}}{2(1-rh)}$$

and corresponding eigenvectors

$$v_A^{\pm} = \left((1-rh)\sqrt{1-h^2},\ rw\sqrt{1-h^2} \pm \sqrt{(1-r^2)(\alpha(r,h)^2-w^2)}\right)^{\top},$$

where $\alpha(r, h)$ was defined in (18). The system is physical and hyperbolic under the conditions $|h| < 1$ and, in agreement with (18), $|w| < \alpha(r, h)$.

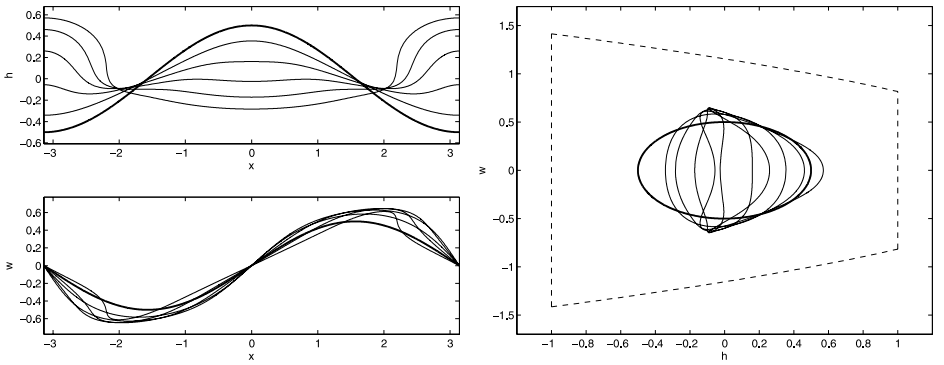

Figure 4. Sloshing solution of (20) for $r = 0.5$ up to breaking time.

A physical realization in which $q'(t)$ and q are zero is the sloshing between two vertical sidewalls. Consider a domain between two vertical sidewalls at $x = 0$ and $x = \pi$. Sloshing implies that $w = 0$ at the walls, and it follows from (14) and (15) that $h_x = 0$ at the walls. Consequently, if one considers an even extension of h and an odd extension of w on the periodic domain $[-\pi, \pi)$, the boundary conditions at $x = 0$ and $x = \pi$ are satisfied, and the solution is represented as a closed curve in phase space. Thus it suffices to employ periodic boundary conditions on this extended domain, together with initial data satisfying the conditions above. A sloshing solution of (20) with $r = 0.5$ up to breaking time is shown in Figure 4. Note that the shape of the hyperbolic region has changed from the Boussinesq case. The case where the lower (heavy) fluid is shallower is initially stabilized by non-Boussinesq effects and instabilities are more likely when the lower fluid is deeper. This can be seen directly from (18), because for $h > r$, the stability region becomes thinner in the w direction. Figure 5 confirms that q for this solution, obtained by evolving (16) independently, remains within machine accuracy as expected.

In Figure 6, another sloshing solution with initial data near a boundary of the hyperbolic region is shown. In this case, the solution curves leave the hyperbolic region and exhibit numerical oscillations typical of an initial-value numerical computation of an elliptic, ill-posed problem. In [6], it was shown that a necessary condition for a quasi-linear system of mixed type to be nonlinearly stable is that (in the simplest 2×2 case) its eigenvectors are tangent to the boundary of the hyperbolic region. The eigenvectors of (20) on the top and the bottom boundaries are not tangent to the curves $w = \pm\alpha(r, h)$, explaining the system's lack of nonlinear stability. (Incidentally, even though we are unable to determine the Riemann invariants of (20) in closed form, we still can conclude that $\lambda_A^{\pm}$ are not smooth functions of the Riemann invariants.) The next section examines whether there is a subregion *inside* the hyperbolic

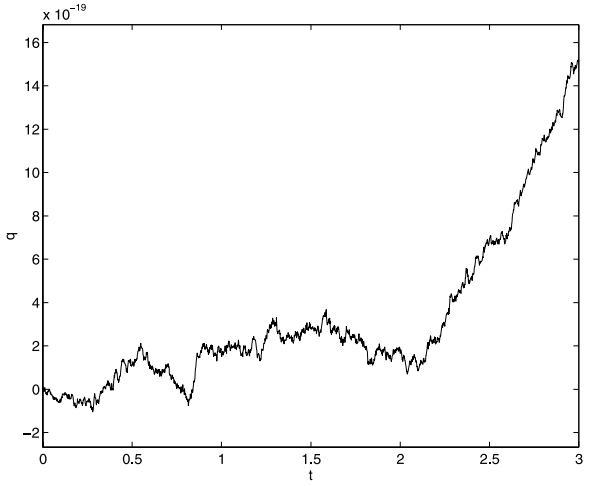

Figure 5. Evolution of $q(t)$ for sloshing solution.

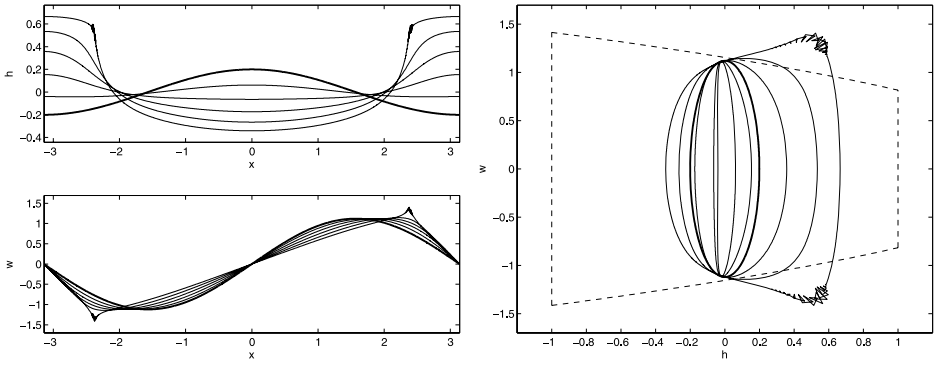

Figure 6. Sloshing solution of (20) for $r = 0.5$ with initial data near boundaries of the hyperbolic region; the numerical solution is of course unreliable outside the hyperbolic region.

region of (20) with the property that any solutions evolving from initial data inside that region remain inside—hence stable—throughout their evolution.

In Figures 7 and 8, the computation of a general periodic solution for which q does not remain zero is shown. Our observations are that even if r is relatively large—the case of $r = 0.5$ corresponds to fluids whose densities differ by a factor of three—the change in q is often small. Both "stable" and "unstable" solutions have been computed in this case also.

4. Simple waves and stable regions

Consider the cases where q and q' are zero. The goal here is to obtain *a priori* bounds on the solutions to (20) and use those to ensure nonlinear stability. For

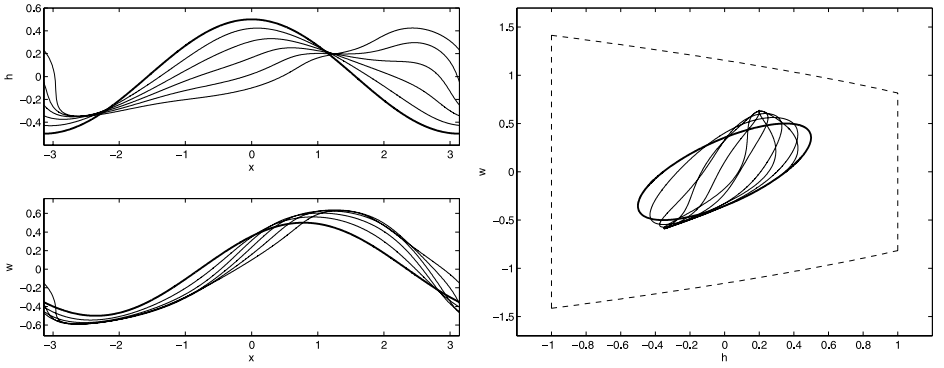

Figure 7. Typical solution of (20) for $r = 0.5$ up to breaking time.

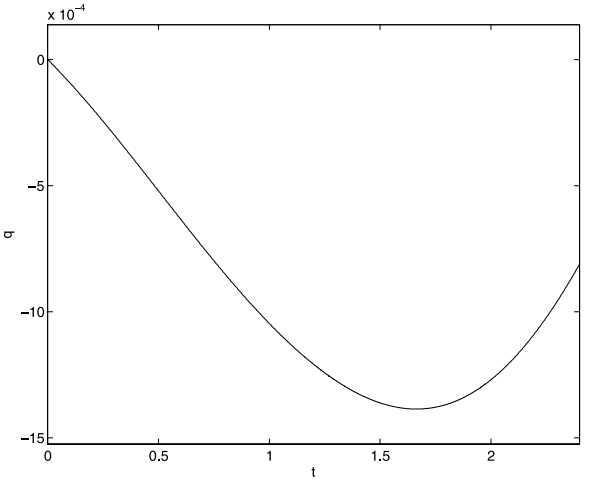

Figure 8. Evolution of $q(t)$ for general periodic data.

this purpose, the notion of simple waves [8, 18] is introduced. *Simple waves* are solutions to (20) of the special form

$$u(x,t) = U(\theta(x,t)), \tag{21}$$

where θ is a scalar function and U is a vector function, both to be determined. Substituting (21) into (20) yields the condition

$$(\theta_t I + \theta_x A(U))\, U'(\theta) = 0,$$

where I is the 2×2 identity matrix. Nontrivial solutions require

$$U' = v(U), \tag{22}$$

and

$$\theta_t + \lambda(U(\theta))\theta_x = 0, \tag{23}$$

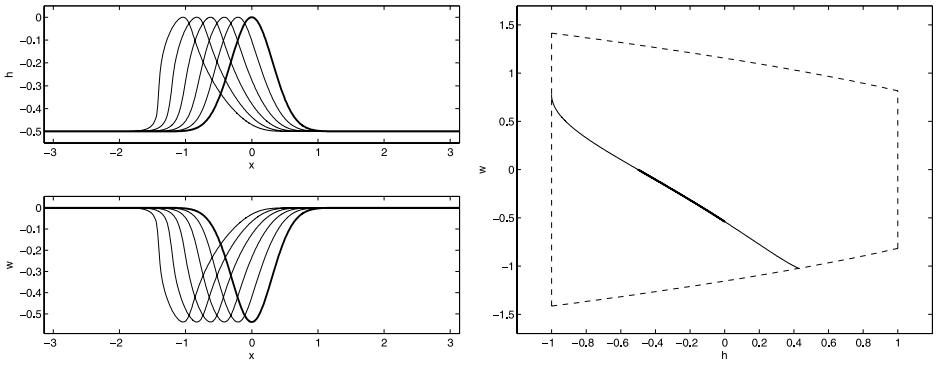

Figure 9. An example of a simple wave. The bold portion of the curve on the right corresponds to the solution shown on the left.

where $v \neq 0$ is an eigenvector of A, and λ is its corresponding eigenvalue. To construct the simple wave, one first solves the system (22) for U, yielding an invariant curve in the phase space parameterized by θ. One can then choose initial data $\theta_0(x)$, which reparameterize the phase space curve with x, and evolve the scalar hyperbolic Equation (23) for $\theta(x, t)$, yielding the solution up to breaking time as a composition of U and θ. Alternatively, one may instead evolve the system (20) directly from the initial data given by $u_0(x) = U(\theta_0(x))$. We show the second construction in Figure 9. The initial data are closed curves lying entirely on an invariant curve U. Note that the solution remains on U throughout its evolution as expected.

We focus here on the curve U rather than on actual simple waves and use the term simple wave to refer to this curve. Through each point in the hyperbolic region of (20), there are two simple waves corresponding to the two vector fields given by the linearly independent eigenvectors. Examples of simple waves are shown in Figure 10. These simple waves are tangent to the left and the right boundaries, which is to be expected as their directions are determined by their corresponding eigenvectors.

Simple waves bound nonsimple solutions in phase space. At each point where a smooth solution curve (in the phase space) is tangent to a simple wave, it behaves locally as the simple wave and hence must evolve along the simple wave rather than cross it. A more rigorous justification is as follows: because u_x is tangent to the solution curve in phase space, it is also tangent to the simple wave at the point where the solution curve is tangent to the simple wave. As a result, u_x is in an eigenspace of A, and so is $u_t = -Au_x$. Thus, one can conclude that the point u remains on the simple wave. Using this idea, one can now understand the behavior shown in Figures 4 and 6. Because the initial curve in Figure 4 can be bounded by four simple waves as shown in Figure 11(a), the resulting solution remains within this bounded region inside

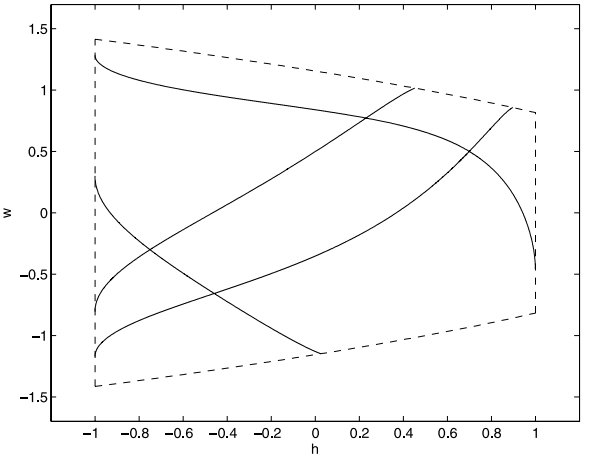

Figure 10. Four simple waves in phase space for $r = 0.5$.

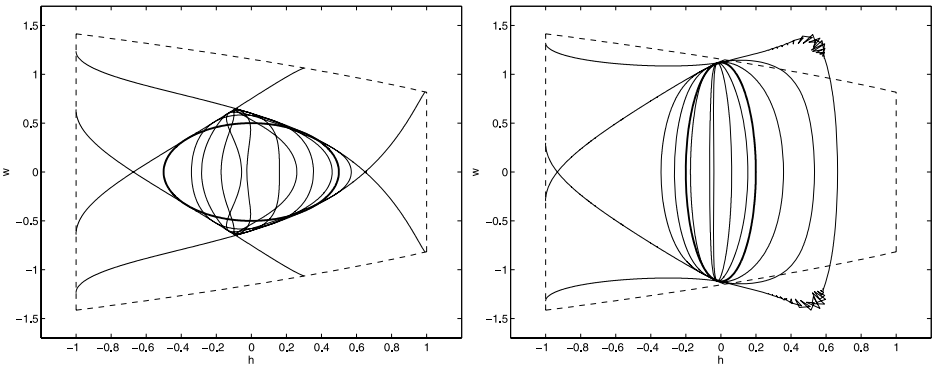

(a) bounding simple waves (b) non-bounding simple waves

Figure 11. Examples of initial data with bounding and non-bounding simple waves.

the hyperbolic region. On the contrary, the initial curve in Figure 6 cannot be bounded by simple waves as shown in Figure 11(b), and the resulting solution is able to leave the hyperbolic region. As it may be difficult to distinguish between solution curves and simple waves in Figure 11(b), another plot without the solution curves and an enlargement of a small neighborhood near the elliptic boundary are shown in Figure 12(a) and (b), respectively. In general, one can determine whether given initial data could be bounded by simple waves by looking at all the simple-wave tangencies of the initial data and constructing a bounding region. This yields *a priori* bounds on the solution of the quasi-linear hyperbolic system (20). In Figure 11(a) and (b), there are four tangencies which lead to simple-wave curves.

Greater care is needed when considering u_x on curves that locally resemble line segments as shown in Figure 13(a), because u_x vanishes on their tips and

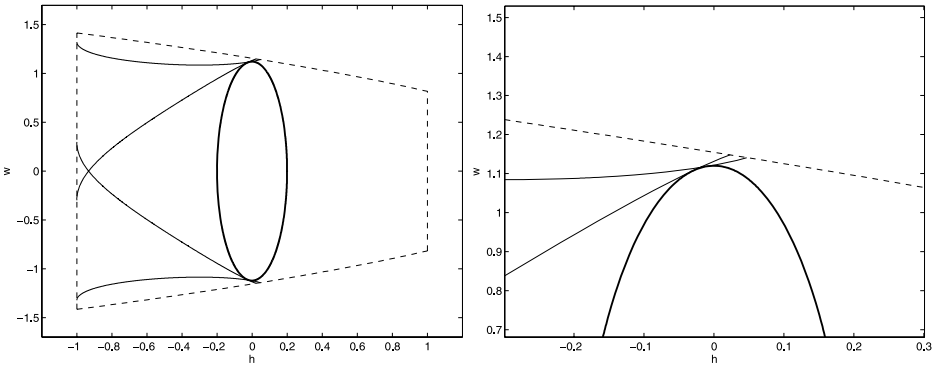

(a) initial data and simple waves (b) enlargement of a small neighborhood

Figure 12. Detail of Figure 11 (b) without solution curves.

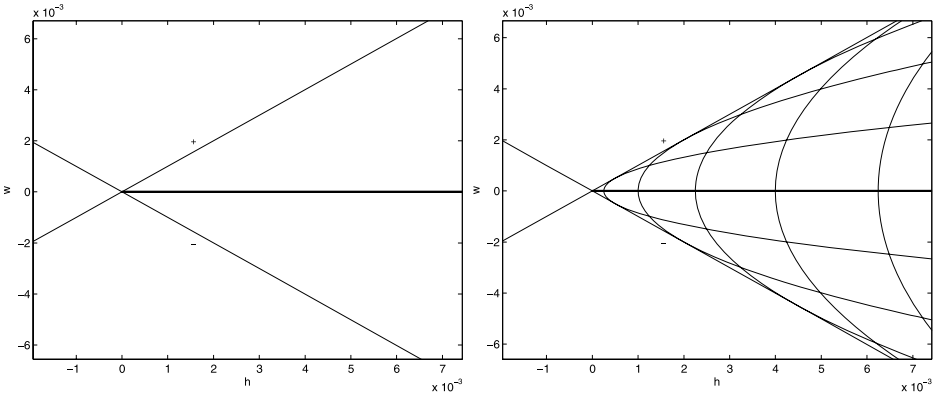

(a) initial curve and simple waves (b) solution curves

Figure 13. The evolution of initial data from a corner formed by simple waves.

the preceding argument on the evolution of u fails. This is generically the case at "corners" of possible simple-wave bounding regions. A local argument for bounding solutions in such a situation is as follows. For simplicity, consider one tip of an initial curve at $u = 0$ corresponding to $x = 0$ and $t = 0$. Through this tip are two simple waves, which resemble lines in the tip's vicinity. Take the directions marked with $+$ and $-$ signs on the simple waves as the directions of eigenvectors v_A^+ and v_A^-, respectively, of A at $u = 0$. For x and t close to 0, one can make the approximation

$$u(x, t) = x^2 a + xtb + t^2 c, \tag{24}$$

where $a, b, c \in \mathbb{R}^2$. (There cannot be a first-degree term in x, because the initial curve must backtrack over itself at the tip. Similarly, there cannot be a first-degree term in t, because $u_t = -Au_x = 0$ at the tip.) It is easily seen that a points in the direction of the initial curve. Substituting u from (24) in

(20), one has $b = -2Aa$ and $c = A^2a$. Consequently, $u = (xI - tA)^2a$. Now, consider everything with respect to a new basis $\{v_A^+, v_A^-\}$. Then A is diagonal, and $a^\top u = ||(xI - tA)a||^2 \geq 0$. This means that each solution curve is a parabola bounded by the + and − rays and tangent to both rays as shown in Figure 13(b), concluding the proof of bounding in this situation.

Instead of considering a bounding region for each initial data, one may find the *largest* subregion inside the hyperbolic region with the property that any solutions evolving from initial data inside this region remain in it. We refer to this region as the *stable region*. The stable region extends to the left and the right boundaries of the hyperbolic region, because these boundaries are simple waves themselves. Because the problem with $q = 0$ in phase space is symmetric with respect to the line $w = 0$, one needs only to find the upper boundary of the stable region, that is, the uppermost simple wave extending from the left to the right boundaries and within the hyperbolic region. This simple wave, denoted by $w = \Gamma(r, h)$, satisfies the equation

$$\frac{dw}{dh} = \frac{rw\sqrt{1-h^2} - \sqrt{(1-r^2)(\alpha(r,h)^2 - w^2)}}{(1-rh)\sqrt{1-h^2}}; \tag{25}$$

that is, its direction is determined by v_A^-. The boundary condition is that it meets the top right corner of the hyperbolic region: $w = \alpha(r, 1)$ for $h = 1$. (One can argue to exclude the other possibility, that the curve terminates at the top left corner, by contradiction.) At this corner (25) is singular, and local analysis shows that the simple wave can be approximated by a line, that is,

$$w - \alpha(r, 1) = \frac{-1 - 3r + \sqrt{(1+r)(1+7r)}}{2(1-r)\sqrt{1+r}} \cdot (1-h) + o(1-h).$$

Thus, the sharp stability (or long-time well-posedness) result of this paper can be stated as follows:

> For the shallow-water system (20) at a fixed value of the Boussinesq parameter r, initial data inside the region $S_r = \{(h, w): -1 \leq h \leq 1 \text{ and } -\Gamma(r, h) \leq w \leq \Gamma(r, h)\}$ is globally well posed, and the solution will remain inside that region for up to breaking. Thus, data inside this region do not trigger large-scale shear instabilities.

Figure 14 shows the stable region within the hyperbolic region for $r = 0.5$. We also show using dotted lines the hyperbolic (and, equivalently, stable) region for the Boussinesq limit for comparison. Note that the stable region of the Boussinesq system is larger than that of the general case, but there is a small region for thin lower layers where non-Boussinesq is stable to larger shear.

In the case where the equations are nonlocal ($q'(t) \neq 0$), a similar result cannot be obtained. However, our numerical experiments show that the induced

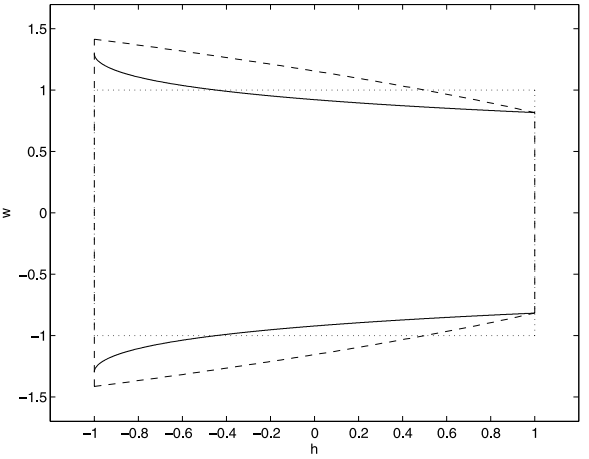

Figure 14. The stable region for $r = 0.5$ is bounded above and below by the solid curve. The dashed curve is the boundary of the non-Boussinesq hyperbolic region, and the dotted curve is the boundary of the hyperbolic region for the Boussinesq approximation.

mean flow q appears always to be very small and seems to affect the results mentioned here only mildly.

5. Conclusion

We have considered in detail the two-layer shallow-water limit. In the Boussinesq approximation, the dynamics is simple to characterize. Initial data with sufficiently large Richardson number everywhere remain stable—a term used here in the sense of well-posedness—until breaking. The non-Boussinesq case is more complicated. First, the evolution equations may be nonlocal depending on the boundary conditions, and second not all initially hyperbolic or wave-like evolution remains as such. There exist initial data that become ill posed after a finite time, indicative of an explosive shear instability. One can, however, *guarantee* long-time well-posedness by choosing initial data within a region bounded by simple waves. In general, simple waves are a powerful means to find *a priori* bounds on the solutions.

A principal practical result of our work is the conclusion that the Boussinesq approximation tends to "stabilize" the ill-posedness due to the KH instability in this setting unless the lower layer is considerably thinner than the upper layer. An interesting future line of work would be to compare the shallow-water dynamics studied here to fully two-dimensional solutions of two-layer Euler's equations. In particular, one would like to observe whether there is a clear physical manifestation of solutions entering the elliptic region.

Acknowledgment

This research was supported by the Division of Mathematical Sciences of the National Science Foundation under grant NSF-DMS-0908077.

References

1. J. Bona, D. Lannes, and J.-C. Saut, Asymptotic models for internal waves, *J. Math. Pures Appl.* 89:538–566 (2008).
2. W. Craig, P. Guyenne, and H. Kalisch, Hamiltonian long-wave expansions for free surfaces and interfaces, *Commun. Pure Appl. Math.* 58:1587–1641 (2005).
3. R. Long, Long waves in a two-fluid system, *J. Meteorol.* 13:70–74 (1956).
4. P. Guyenne, D. Lannes, and J.-C. Saut, Well-posedness of the Cauchy problem for models of large amplitude internal waves, *Nonlinearity* 23:237–275 (2010).
5. D. Bresch and M. Renardy, Well-posedness of two-layer shallow-water flow between two horizontal rigid plates, *Nonlinearity* 24:1081–1088 (2011).
6. L. Chumakova, F. E. Menzaque, P. A. Milewski, R. R. Rosales, E. G. Tabak, and C. V. Turner, Stability properties and nonlinear mappings of two and three-layer stratified flows, *Stud. Appl. Math.* 122:123–137 (2009).
7. P. A. Milewski, E. G. Tabak, C. V. Turner, R. R. Rosales, and F. E. Menzaque, Nonlinear stability of two-layer flows, *Commun. Math. Sci.* 2:427–442 (2004).
8. P. Lax, Hyperbolic systems of conservation laws, *Commun. Pure Appl. Math.* 10:537–566 (1957).
9. H. Lamb, *Hydrodynamics*, Dover, New York, NY, 1945.
10. D. J. Benney, Long nonlinear waves in fluid flows, *J. Math. Phys.* 45:52–63 (1966).
11. R. Camassa and W. Choi, Fully nonlinear internal waves in a two-fluid system, *J. Fluid Mech.* 396:1–36 (1999).
12. R. Camassa, W. Choi, H. Michallet, P.-O. Rusas, and J. K. Sveen, On the realm of validity of strongly nonlinear asymptotic approximations for internal waves, *J. Fluid Mech.* 549:1–23 (2006).
13. D. M. Holland, R. R. Rosales, D. Stefanica, and E. G. Tabak, Internal hydraulic jumps and mixing in two-layer flows, *J. Fluid Mech.* 470:63–83 (2002).
14. T. Jacobsen, P. A. Milewski, and E. G. Tabak, Mixing closures for conservation laws in stratified flows, *Stud. Appl. Math.* 121:89–116 (2008).
15. A. D. D. Craik, *Wave Interactions and Fluid Flows*, Cambridge University Press, Cambridge, UK, 1988.
16. R. Liska, L. Margolin, and B. Wendroff, Nonhydrostatic two-layer models of incompressible flow, *Comput. Math. Appl.* 29:25–37 (1995).
17. L. C. Evans, *Partial Differential Equations*, AMS, Providence, RI, 2000.
18. L. Chumakova and E. G. Tabak, Simple waves do not avoid eigenvalue crossings, *Commun. Pure Appl. Math.* 63:119–132 (2010).

University of Wisconsin-Madison

(Received April 5, 2011)